An Evaluation of Solid-State LiDAR for Localization and HD point cloud mapping

Yang-En Lu [1 *], Kai-Wei Chiang[1], Meng-Lun Tsai [2], Yu-Ting Chiu [2], Surachet Srinara [1], Ting-Chun Wu [2], N. El-Sheimy[3]

[1] Dept. of Geomatics, National Cheng Kung University, Tainan, Taiwan – kwchiang@geomatics.ncku.edu.tw, luyangen124@gmail.com, surachetsrinara@gmail.com

[2] High Definition Map Research Center, Dept. of Geomatics, National Cheng Kung University, Tainan, Taiwan – taurusbryant@geomatics.ncku.edu.tw, p66081106@gs.ncku.edu.tw, 11109070@gs.ncku.edu.tw

[3]Dept. of Geomatics Engineering, The University of Calgary, 2500 University Dr NW, Calgary AB T2N 1N4, Canada – elsheimy@ucalgary.ca

KEY WORDS: Mobile Mapping**,** solid-state LiDAR, LiDAR Odometry, point cloud map, localization

ABSTRACT:

Cost-effective navigation and positioning systems for autonomous vehicles has become a key focus of research in recent years. Having an accurate position within a lane is vital to enabling high levels of automation and improving safety. Traditionally, vehicle navigation and positioning systems have relied heavily on the Global Navigation Satellite System (GNSS), particularly in open-sky scenarios. However, GNSS signals can be easily disrupted by environmental interferences. These include phenomena such as urban canyons, which result from multi-path interferences, as well as challenges posed by Non-Line-of-Sight (NLOS) situations. In the pursuit of developing robust systems resilient to such issues, the concept of sensor fusion has been widely employed. Among all sensors used in commercial self-driving vehicles, mechanical LiDAR is the primary sensor. Utilizing point cloud data from LiDAR and registering it with a prior point cloud map can result in highly accurate position results. However, the high cost of mechanical LiDAR has limited the mass production of point cloud map and autonomous vehicle. In this paper, we evaluate several successful Simultaneous Localization and Mapping (SLAM) architectures from LiDAR-based to LiDAR-Inertial-based using single Solid-State LiDAR (SSL). Last, we proposed a single SSL mapping and localization framework that can achieve 36 centimeters 3D RMSE and 0.5 degree accuracy in heading estimation.

1. INTRODUCTION

The multi-sensor fusion approach has gained significant popularity in recent times due to its enormous potential to provide accurate navigation data for advanced applications such as automated driving systems (ADS) and mobile mapping systems (MMS) (Chiang et al., 2019). In traditional navigation methods, reliance was primarily placed on Global Navigation Satellite Systems (GNSS) (Noureldin et al., 2013) and Inertial Navigation System (INS) (Nassar, 2003). However, INS is susceptible to position error accumulation over time. To mitigate this limitation, GNSS solutions can be used to constrain position error of INS, thereby improving the robustness of the navigation solution. Despite the benefits of loosely-coupled (LC) integration schemes, LC is vulnerable to rejecting bias GNSS solutions, particularly in challenging environments such as those with multipath effects or long-term signal outages. Consequently, the fusion solution can become biased by these measurement updates. Therefore, it is crucial to consider adding aided sensors and prior maps to improve localization accuracy and robustness.

In recent years, there has been a focus on comparing the characteristics of various extrinsic sensors for autonomous vehicles. One commonly used sensor is the visual sensor, which is known for being cost-effective. It operates well in texture environments. However, it is not efficient in bad weather conditions or low lighting, which limits its usability. Another sensor option is radar, which is also capable of achieving high-performance object detection and tracking tasks, particularly at 77GHz mm-Wave frequency. However, the radar sensor's high price and low spatial resolution compared to other sensors pose challenges for its widespread adoption. On the other hand, the LiDAR sensor offers robustness with a long detection range and outstanding spatial resolution. These qualities make LiDAR sensors invaluable for SLAM applications, enabling superior localization and precise mapping with loop closure. LiDAR has been extensively utilized in mobile vehicles for over two decades due to its reliability and performance. However, the cost of traditional mechanical LiDAR systems has been a limiting factor in their mass production and widespread use. Fortunately, solid-state LiDAR has recently been released commercially, and it offers reliable performance at a much lower cost compared to mechanical LiDAR (Nam and Gon-Woo, 2021). As such, solid-state LiDAR is expected to play an increasingly important role in the development of advanced navigation and mapping technologies in the years to come. In the state of the art, Simultaneous Localization and Mapping (SLAM) frameworks have successfully operated by using solid-state LiDAR which are LiDAR Odometry and Mapping (LOAM) (Zhang and Singh, 2017), FAST-LIO2 (Xu et al., 2021) and SC-FAST-LIO (Kim et al., 2021). State-of-the-art LiDAR SLAM algorithms often use the drift rate or closing error to assess the accuracy of mapping and localization. However, these measures are impractical for large-scale outdoor mapping applications because they require the mobile mapping platform to return to the same closure point, which is often not feasible. Moreover, the mapping results of SLAM are typically not in a global coordinate system like WGS84, making it challenging to integrate with INS/GNSS navigation systems. Therefore, this paper raises three contributions as follows:

1) Evaluate the state-of-the-art LiDAR SLAM using single solid-state LiDAR by using navigation-grade INS/GNSS navigation system.

* Corresponding author

2) Propose a single solid-state LiDAR mapping scheme that can produce high quality and density point cloud map which could be used as prior map for the proposed integration scheme.
3) Propose an INS/GNSS/SSL integrated scheme that can improve navigation accuracy by utilizing a prior point cloud map produced from the mapping scheme proposed in this paper.

2. EVALUATION OF SLAM FRAMEWORK USING SSL

In this section, we delve into three successful SLAM frameworks that utilize solid-state LiDAR. These systems encompass a purely LiDAR-oriented approach, a fusion of LiDAR and inertial sensors, and a variant that incorporates scan-context assistance with loop-closure to reduce the drift of LiDAR odometry. To evaluate the performance of state-of-the-art SLAM framework, we establish an evaluation scheme illustrated in Figure 1. The proposed scheme can be divided into three main steps: (1) time synchronization (2) SSL SLAM and georeferencing (3) reference solution and error analysis. To enable comparison of the results with the reference system, it is imperative to synchronize the time systems. In this study, we employed a time synchronization board to rectify the clock bias and synchronize the board's clock with GPS time. Subsequently, the board was designated as the master clock and transmitted the Precision Time Protocol (PTP) to the local network. The Industrial Personal Computer (IPC), which supports PTP hardware synchronization function, was synchronized with the master clock. In other words, the IPC time was set to GPS time. Finally, each sensor connected to the IPC was time-synchronized.

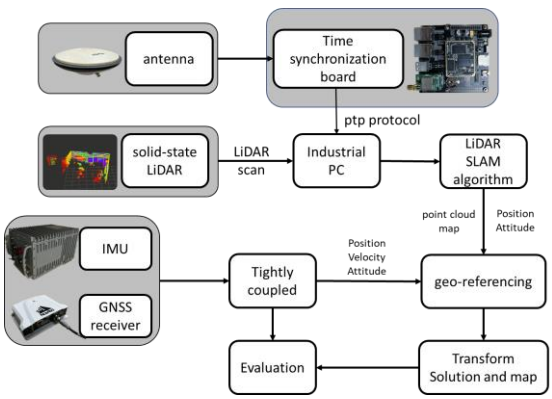

Figure 1. The evaluation scheme of LiDAR SLAM

2.1 Low-drift and real-time LiDAR odometry and mapping

Low-drift and real-time LiDAR odometry and mapping represents an innovative use of Light Detection and Ranging (LiDAR) technology to capture environmental data and translate it into three-dimensional maps. LiDAR employs laser beams to measure distances to objects and surroundings, offering highly accurate data. Low-drift indicates the precision of this technology, particularly over extended periods of usage. Its understanding of the environment does not deviate significantly from reality. This is accomplished through a technique called loop closure detection, which identifies and corrects inconsistencies in the map and accumulated navigation errors. At the same time, real-time suggests that LiDAR data can be processed immediately for the creation or updating of maps. For applications requiring instant feedback, such as autonomous vehicles and drones, this immediacy is vital. With such technology, vehicles or drones can build and update their understanding of the environment while on the move, ensuring the safety and efficiency of their paths. Therefore, the low-drift and real-time LiDAR odometry and mapping technology offers a powerful and accurate means of instantaneously creating and updating precise environmental maps. It significantly reduces navigation errors, which is essential for many modern technologies, particularly in the fields of autonomous driving and robotics.

In our evaluation of LOAM, represented in Figure 2, experimental data suggests that LOAM exhibits optimal performance when utilizing SSL under conditions of low velocity. However, the system displays noticeable inadequacy when operated at high speeds and high rate turning. The comprehensive point cloud map, depicted in the right of Figure 2, substantiates the assertion that using a solitary SSL unit allows us to attain approximately 3980 data points per cubic meter. This measurement is obtained after the procedure of ground point extraction has been executed. The generated map displays a relatively high data density, especially when juxtaposed with a map generated using a traditional mechanical LiDAR system. This comparative analysis underscores the effectiveness of solid-state LiDAR in generating detailed and dense mapping data, thereby highlighting its utility in applications requiring a high level of precision.

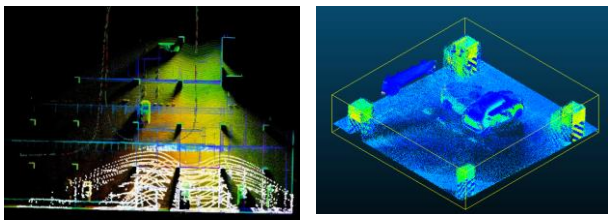

Figure 2. (Left) The real-time mapping result (Right) The point cloud map of a single block in underground parking lot.

2.2 FAST-LIO

The FAST-LIO algorithm was specifically designed for use with solid-state LiDAR. The use of solid-state LiDAR presents unique challenges for SLAM, such as the fact that LiDAR measurements typically reflect the geometric structures within an environment. When these strong features are absent, the LiDAR-based system can easily deteriorate. This problem becomes even more pronounced when the LiDAR has a limited field of view. LiDAR scans usually generate numerous feature points, often amounting to several thousand due to the high-resolution scanning. However, reliance on these feature points alone can fall short in circumstances where the system starts to deteriorate, and achieving accurate pose estimation becomes problematic. On the other hand, merging such a significant volume of feature points with IMU measurements in a tightly integrated manner can demand substantial computational power. Further, the technique of sequentially sampling laser points in a LiDAR scan, through the use of several laser/receiver pairs, can create motion distortion, significantly compromising the precision of scan registration. Therefore, addressing this motion distortion caused by sequential laser point sampling is an essential factor when integrating LiDAR with inertial measurements. In order to enable effective LiDAR navigation in high-speed and dynamic situations, the FAST-LIO has been introduced. This is a powerful and efficient algorithm for LiDAR-inertial odometry. Specifically, this algorithm is designed to perform well in high-motion situations or in environments that are noisy, cluttered, or where system degeneration occurs. It uses a tightly-coupled iterative Kalman filter for fusing LiDAR feature points with IMU measurements, and it employs a thorough back-propagation method to compensate for any motion distortion.

The results of the FAST-LIO experiment are illustrated in Figure 3. These results show that the algorithm can function effectively

under high-speed scenarios and prove to be much more robust than the LiDAR-only SLAM scheme. However, the trajectory and map of FAST-LIO still tend to drift over distance. The average vehicle speed during the highway experiments was approximately 110 km/hr.

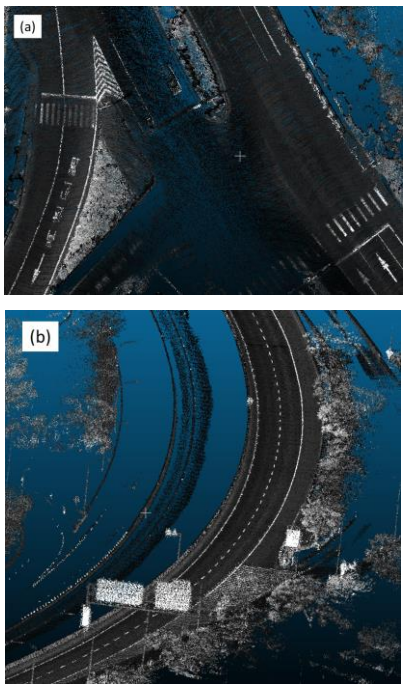

Figure 3. This is the mapping result of (a) interchange and (b) curve on Highway 8.

2.3 SC-FAST-LIO

SC-FAST-LIO is an algorithm that integrates FAST-LIO2 and scan context-based loop detection with pose-graph optimization. The flowchart diagram is shown in Figure 4.

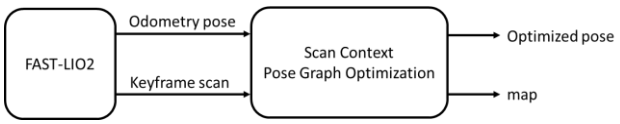

Figure 4. The flowchart of SC-FAST-LIO

Scan Context is a strategy used within SLAM systems to assist in detecting loop closures. In other words, it helps the system identify when it has returned to a location it has visited before, which is important for correcting any accumulated positioning errors. This method is particularly used with LiDAR-based SLAM systems. It involves transforming a 3D LiDAR scan into a 2D image-like representation, called a scan context. This 2D scan context essentially holds a summary of the unique environmental features captured by the LiDAR scan. The advantage of Scan Context lies in its simplicity and efficiency, as well as its robustness. Even though the method is simple, it can produce high-quality results even in complex environments. It's especially useful for large-scale or long-term SLAM operations, where efficient and robust detection of loop closures is critical.

The results of SC-FAST-LIO are illustrated in Figure 5. The point cloud map shows that the loop-closure can constrain the drift in vertical direction. The point cloud map demonstrates that loop-closure can mitigate the drift in the vertical direction. Additionally, owing to the support from the SSL's internal IMU, the height variance scenario still performs well in such circumstances.

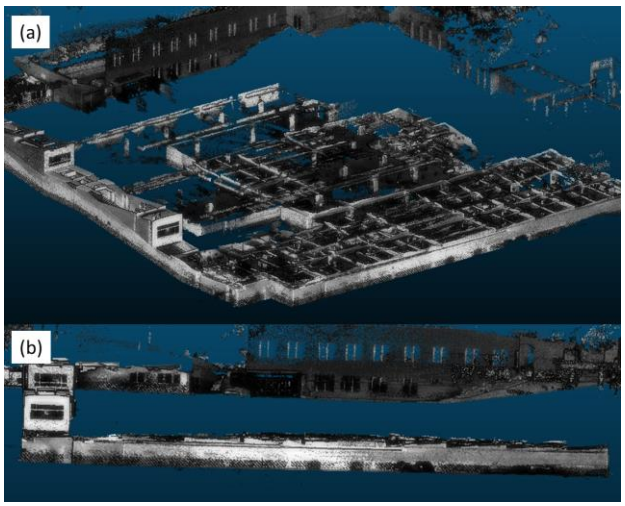

Figure 5. Underground parking lot point cloud map (a) The perspective from a 45-degree angle from above (b) Side view

3. PROPOSED SINGLE SSL MAPPING SCHEME

In the state-of-the-art LiDAR SLAM algorithm, the use of the LiDAR-inertial method enables localization and mapping in high-speed and high-dynamic motion scenarios. To control the drift in the vertical direction, it's necessary to perform a scan context loop closure. However, this loop closure criterion requires the mapping platform to scan the same direction multiple times, which can be time-consuming. Furthermore, the LiDAR-SLAM point cloud map is defined under local defined mapping frame which is not practical to fuse with INS/GNSS system. To accelerate the mapping process time and provide a prior map for INS/GNSS integration system. We proposed a single solid-state LiDAR mapping scheme. The scheme consists of three remarkable steps: Time synchronization and motion distortion compensation, pose from INS/GNSS tightly coupled integration system and direct georeferencing. The proposed mapping scheme is shown as Figure 6. The first step is to rectify the clock bias and synchronize the board's clock with GPS time. Then, we utilize the Livox LiDAR internal IMU to compensate the motion distortion by using FAST-LIO2 algorithm. The output from the above procedure is the undistorted point cloud. For the second step, the LiDAR data and INS/GNSS navigation solution has to be the same time domain and then interpolate the navigation information. Finally, the direct georeferencing of LiDAR measurements is conducted regarding a pose obtained from previous step. While direct georeferencing requires the information of boresight angle and lever-arm. These two parameters play an important role in point cloud mapping.

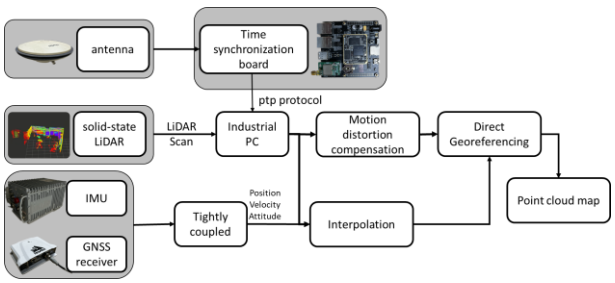

Figure 6. The single LiDAR mapping scheme

3.1 INS/GNSS integration system

An Inertial Navigation System (INS) is a self-reliant system capable of continuously providing Position, Velocity, and Attitude (PVA) solutions. The INS consists of an Inertial

Measurement Unit (IMU), a navigation algorithm, and a computer that runs the algorithm. The system utilizes a trio of gyroscopes and accelerometers. The INS algorithm operates through an integration process that first detects acceleration, then integrates this data to calculate velocity and displacement. With advancements in Micro-Electro-Mechanical Systems (MEMS) technology, we now have entire inertial units built into a single chip, equipped with multiple integrated MEMS accelerometers and gyroscopes. These systems are not only compact and easily portable, but their cost is also significantly lower than high-quality INS.

On the other hand, the Global Positioning System (GPS) provides an alternative navigation method. A GPS receiver gives position and velocity measurements, or more specifically, pseudorange, carrier phase, and Doppler. Unlike INS estimates, the accuracy of GPS measurements is time-independent with bounded errors. However, the accuracy of GPS measurements can be compromised due to factors such as weak signal strength, the length of the PRN code, tracking loop errors, multi-path effects, variations in satellite geometry, and receiver clock instability. Furthermore, traditional GPS positioning faces challenges in environments like areas under dense foliage, urban canyons, and indoor settings, especially with the rising demand for more diverse applications. In addition to the results from the TC-INS/GNSS integration system (), the navigation solution was further refined using a forward and backward smoothing process. (Shin, 2005).

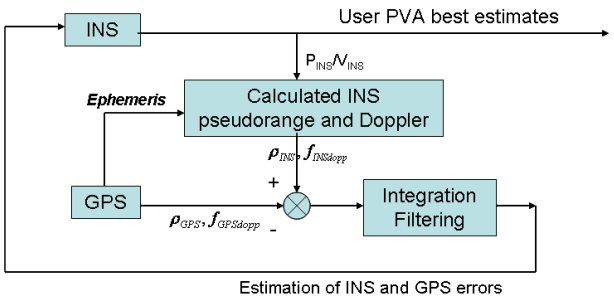

Figure 7. INS/GNSS tightly coupled integration (El-Sheimy, 2006)

3.2 LiDAR-IMU Calibration and Direct Georeferencing

Before direct georeferencing, the geometric relationship between the IMU and LiDAR must be established. This relationship can be characterized using a translation vector, known as the lever-arm, and three rotation angles, commonly referred to as the boresight angles. The calibration method is based on prior high-definition point cloud map (Srinara et al., 2022). This calibration method is based on expressing the mounting parameters within the direct georeferencing equation for each epoch time and conditioning a set of INS/GNSS and LiDAR navigation solutions to lie on it. There is no need for a required information about the planar features in the calibration field as part of the unknowns. Such conditions are only benefitable in the residential area where the presence of sufficient planes in form of building is abundant.

Direct georeferencing of LiDAR measurements is a common method used to transform LiDAR points, which are defined in their own coordinate system, into a mapping coordinate system. The mapping coordinate system often uses a local level frame that typically aligns with the East-North-Up or North-East-Down direction. Figure 8 demonstrates the geometric relationship among the navigation sensory components based on the land vehicular system in this paper. These sensory relationships are used to construct the formula called the direct geo-referencing (DG). To estimate the navigation states based on LiDAR scan through the scan-to-map approaches, DG in this process involves transforming the coordinates of the current scan in the LiDAR frame (i.e., l-frame) to coordinates in the mapping frame (i.e., m-frame). The DG formula for land vehicular-based mobile navigation and positioning system can be expressed as follows:

$$(r_l^m)_k = (r_b^m)_k + (R_b^m)_k (r_l^b) \quad (1)$$

$$r_p^m = (r_l^m)_k + (R_b^m)_k (R_l^b \cdot r_p^l) \quad (2)$$

where $(r_p^m)_k$ = the coordinates of LiDAR measurement in the m-frame at epoch k.
$(r_l^m)_k$ = the LiDAR's position vector at epoch time k with respect to the m-frame.
$(r_b^m)_k$ = the translation vector at epoch time k for the b-frame with respect to the m-frame.
$(R_b^m)_k$ = the rotation matrix at epoch time k for the b-frame with respect to the m-frame.
$r_l^b \; and \; R_l^b$ = lever-arm and boresight angle.

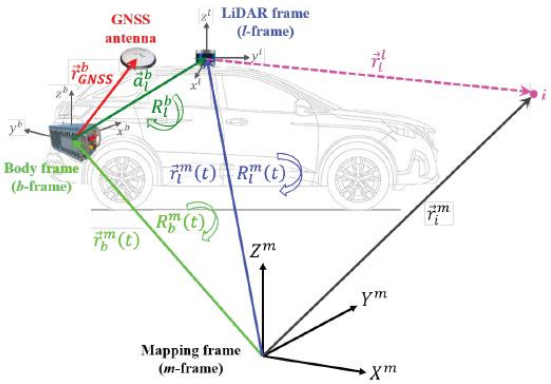

Figure 8. Geometric relationship of navigation sensor (Srinara et al., 2022)

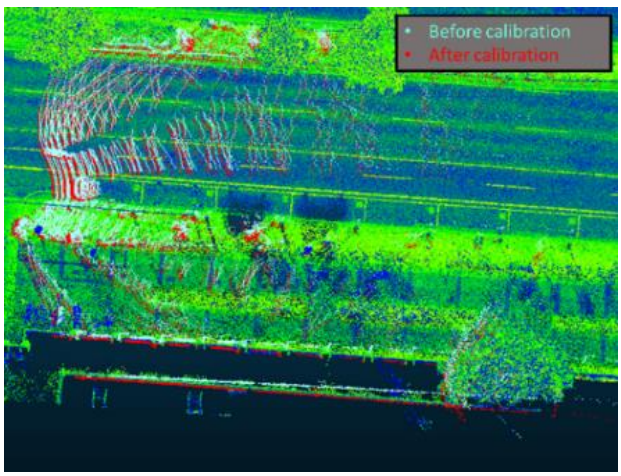

Figure 9. The impact of calibration between the IMU and LiDAR is compared with a prior HD point cloud map.

As depicted in Figure 9, the proper calibration of both the lever-arm and boresight angle plays a crucial role in mapping. Upon correct calibration, the point cloud obtained through direct georeferencing is found to perfectly match with the prior high-definition point cloud map, which was previously created by a professional surveying company. This precision ensures that the transformed data accurately corresponds with the reference data, confirming the successful calibration of the lever-arm and boresight angle. However, the situation drastically changes when the lever-arm and boresight angle are not finely calibrated. In such cases, the map after georeferencing exhibits significant discrepancies when compared to the high-definition point cloud

map. Such inaccuracies are manifested as systematic errors within the mapping outcome, highlighting the crucial need for accurate calibration. If these crucial steps of calibration are not performed meticulously, the reliability and validity of the mapping process can be significantly compromised, potentially leading to errors in further applications of the data.

4. PROPOSED INS/GNSS/SSL INTEGRATED SCHEME

The proposed LiDAR-SLAM-based navigation scheme is illustrated in Figure 10. Here, GNSS refers to the DGNSS with the measurements received from multi-constellation system. The initial guess for NDT scan-matching is derived from INS/GNSS integrated solution. This solution predicts and updates the velocity, position, and attitude information, while simultaneously feeding back the bias and scale factor from the EKF to the INS mechanism. The measurement update incorporates the GNSS position update along with the position and heading from NDT scan-matching.

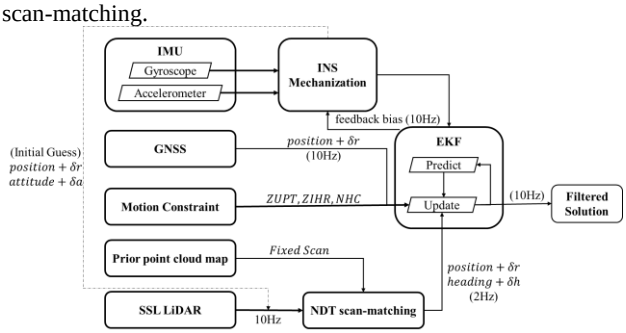

Figure 10. Proposed INS/GNSS/SSL integration scheme

4.1 INS/GNSS integrated solution

In this paper, the INS and DGNSS sensors integration system is developed utilizing the Loosely Coupled (LC) scheme, which needs an optimal estimator to compare the difference between each measurement with predicted variables and establish the error model, to estimate the possible error. The state vector for EKF input is showed in Equation 3.

$$x_k = [r \quad v \quad \varphi \quad b_a \quad b_g \quad s_a \quad s_g]^T \tag{3}$$

where r = the position defined under WGS84.
v = the velocity defines under local level frame.
φ = the attitude which contains roll, pitch and heading.
b_a, b_g = the bias of accelerometer and gyroscope.
s_a, s_g = the scale factor of accelerometer and gyroscope.

5. EXPERIMENT SETUP

A land vehicle-based mobile mapping system is adopted in our case for evaluation of SSL performance in mapping and localization. The hardware setup employed in the experiment is illustrated in Figure 11. In this study. the solid-state LiDAR used to test the proposed INS/GNSS/SSL integrated system is Livox HAP and the INS/GNSS is Novatel PwrPak7D-E2 module. The specification and performance characteristics is shown in Table 2 and Table 3 respectively. To verify the accuracy of the results, we utilized the navigation-grade IMU iMAR iNAV-RQH-10018 and GNSS receiver NovAtel PwrPak-7D as the reference system. The reference solution was post-processed using the commercial software Inertial Explorer. The GNSS/IMU fusion solution used in the experiment was tightly-coupled with forward and backward smoothing process to ensure the highest level of accuracy possible for the results. The reference system IMU specification is shown in Table 1.

Figure 11. mobile mapping platform with sensor configuration

Gyroscope	
Bias instability	<0.002 deg/hr
Angular random walk	<0.0015 $deg/\sqrt{hr}$
Accelerometers	
Bias instability	<10 μg
Velocity random walk	0.0004 m/s/$\sqrt{hr}$

Table 1. IMU specification of iNAV-RQH-10018

Gyroscope	
Bias instability	0.8 deg/hr
Angular random walk	0.06 $deg/\sqrt{hr}$
Accelerometers	
Bias instability	12 μg
Velocity random walk	0.025 m/s/$\sqrt{hr}$

Table 2. IMU specification of PwrPak7D-E2

Specification	Livox HAP
Detection range	150 m @10%
Distance Error	<2 cm
Frame rate	10 Hz
Horizontal FoV	120°
Vertical FoV	25°
Angular Resolution	0.23° (Vertical) × 0.18° (Horizontal)

Table 3. Performance characteristics of Livox SSL

5.1 Experiment Environmental Description

In this study, the experiment was conducted in two distinct scenarios: (1) a high-speed, featureless environment, and (2) a GNSS challenging and outage environment. The first scenario represents the National Highway 8, while the second scenario depicts the area around NCKU, characterized by numerous buildings, trees, and an underground parking lot. The average vehicle speed during the highway experiments was approximately 110 km/hr. The test route is shown in Figure 12:

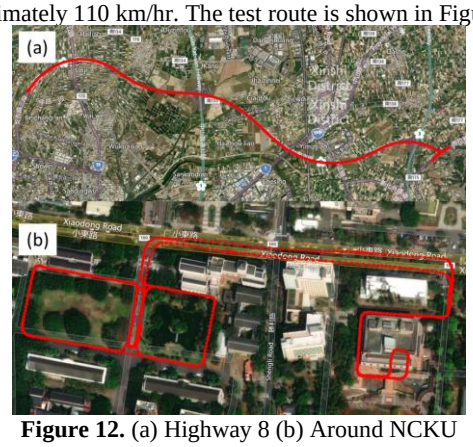

Figure 12. (a) Highway 8 (b) Around NCKU

5.2 Evaluation of state-of-the-art SSL SLAM framework

The following section is divided into two test fields. The distance travelled, defined as the maximum three-dimensional error over the accumulated distance, will also be calculated. This value serves as an index to evaluate the performance of the odometry.

5.2.1 National highway 8

The georeferenced trajectories of each tested SLAM framework are shown in Figure 13. The distance travelled by LOAM is 0.276, by FAST-LIO is 0.044, and by SC-FAST-LIO is 0.043.

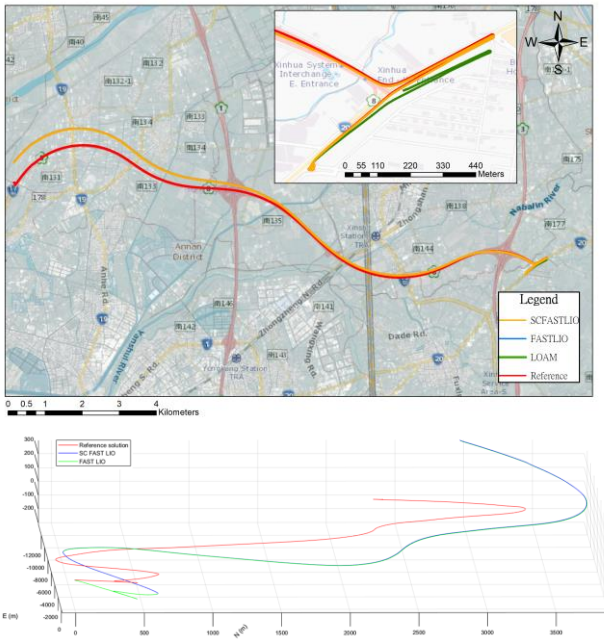

Figure 13. Trajectories of tested SLAM algorithm in highway 8

5.2.2 Around NCKU and its Underground Parking Lot

The georeferenced trajectories of each tested SLAM framework are shown in Figure 14. The distance travelled by LOAM is 0.6, by FAST-LIO is 0.033, and by SC-FAST-LIO is 0.031.

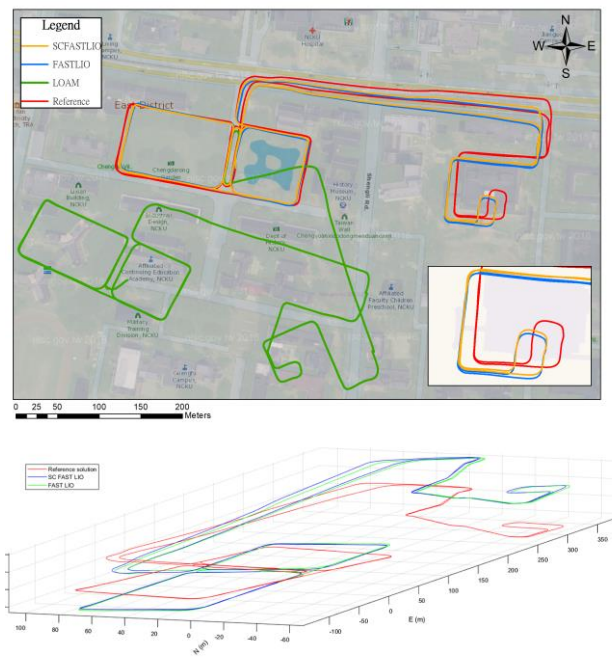

Figure 14. Trajectories of tested SLAM algorithm in NCKU

5.3 Mapping results of proposed mapping scheme

The following section is divided into two test fields, with the mapping results displayed in Figure 15 and Figure 16. As shown below, the point cloud mapping result was remarkably successful. The navigation-grade IMU iMAR iNAV-RQH-10018 was utilized, yielding a high level of detail and accuracy with the use of a single SSL. Each individual point was spatially accurate, contributing to an intricate three-dimensional representation that closely mirrored the real-world structure. The density of the points was optimal, ensuring a high level of detail without becoming overwhelming or unmanageable. Even the subtle details of the original subject were clearly discernible, thanks to the high resolution of the point cloud. The intensity provides additional information, enhancing the overall perception of the subject. These positive results affirm the effectiveness of our point cloud mapping techniques, demonstrating their ability to produce reliable, high-fidelity representations. In the next section, the point cloud map created in this section will be used as the prior map for the proposed algorithm.

5.3.1 National highway 8

Figure 15. Mapping result of National highway 8

5.3.2 Around NCKU and its Underground Parking Lot

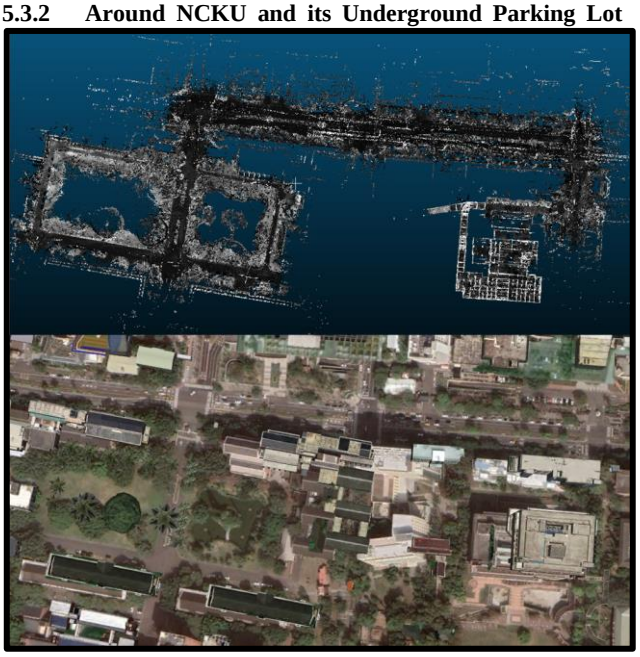

Figure 16. Mapping Results for the Area around NCKU and the Underground Parking Lot.

5.4 Evaluation of proposed integration scheme

In this experiment, a MEMS-grade IMU was chosen as the test subject for our proposed integration scheme. We evaluated three different algorithms: INS/GNSS, SC-FAST-LIO, and our proposed integration scheme. As depicted in Figure 17, the lower image represents an underground parking lot, a typical GNSS-outage area. In such areas, the INS/GNSS solution tends to deviate from the reference solution. Additionally, the left side of the figure shows a GNSS-challenging environment, leading to a degradation in the accuracy of the DGNSS solution. The INS/GNSS system is adversely affected by such poor GNSS measurement updates. However, with our proposed system, it is still possible to maintain decimeter-level position accuracy even in challenging GNSS conditions. When compared to other algorithms, our solution stands out for its robustness and precision.

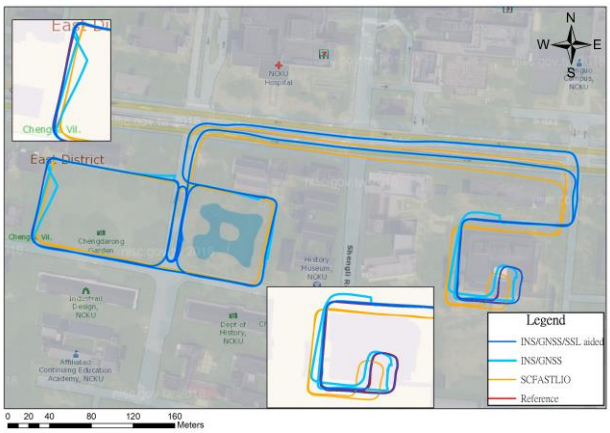

Figure 17. The trajectories of proposed integration scheme, INS/GNSS and SC-FAST-LIO

Unit: Meter	Position Error	East	North	Height
INS/GNSS/SSL	Mean	0.049	0.015	0.019
	STD	0.259	0.250	0.059
	RMSE	0.263	0.251	0.062
INS/GNSS	Mean	-0.402	0.077	-0.197
	STD	1.888	1.523	0.520
	RMSE	1.930	1.525	0.556
SC-FAST-LIO	Mean	-3.722	-4.450	5.287
	STD	5.869	4.050	10.353
	RMSE	6.950	6.018	11.625

Table 4. The error analysis of the positioning error, including INS/GNSS, SC-FAST-LIO, and proposed integration scheme.

6. CONCLUSION

In conclusion, our exploration into LiDAR SLAM algorithms has been extensive and insightful. We discovered that incorporating scan-context significantly improves the LiDAR SLAM's capability to constrain the vertical direction. Among the algorithms tested - LOAM, FAST-LIO, and SC-FAST-LIO - all exhibited a tendency to drift over distance. Nevertheless, SC-FAST-LIO and FAST-LIO performed superiorly compared to LOAM, which is a purely LiDAR SLAM algorithm. However, the scan-context does have its drawbacks; it requires multiple passes in the same direction, which can be inefficient when mapping larger environments. Additionally, it is crucial to transform the mapping coordinate system into a global one, such as WGS84, or a local level frame to simplify fusion with the INS/GNSS system.

To address these challenges, we proposed a novel mapping scheme employing a navigation-grade IMU with a single SSL, which produced highly detailed and dense point cloud maps. This approach, when fused with MEMS-grade IMU, surpasses the performance of both INS/GNSS and SC-FAST-LIO. Furthermore, our proposed integration scheme demonstrated commendable accuracy, achieving an error under 36 cm in 3D. In sum, this study offers a promising trajectory for future research in advanced mapping techniques, with our proposed scheme paving the way for precise, efficient, and high-resolution mapping using solid-state LiDAR.

REFERENCES

Chiang, K.W., Tsai, G.J., Chang, H.W., Joly, C., EI-Sheimy, N., 2019. Seamless navigation and mapping using an INS/GNSS/grid-based SLAM semi-tightly coupled integration scheme. Information Fusion 50, 181–196. https://doi.org/10.1016/j.inffus.2019.01.004

Kim, G., Choi, S., Kim, A., 2021. Scan Context++: Structural Place Recognition Robust to Rotation and Lateral Variations in Urban Environments.

Nam, D. Van, Gon-Woo, K., 2021. Solid-state LiDAR based-SLAM: A concise review and application, in: Proceedings - 2021 IEEE International Conference on Big Data and Smart Computing, BigComp 2021. Institute of Electrical and Electronics Engineers Inc., pp. 302–305. https://doi.org/10.1109/BigComp51126.2021.00064

Nassar, S., 2003. Improving the Inertial Navigation System (INS) Error Model for INS and INS/DGPS Applications.

Noureldin, A., Karamat, T.B., Georgy, J., 2013. Fundamentals of inertial navigation, satellite-based positioning and their integration, Fundamentals of Inertial Navigation, Satellite-Based Positioning and their Integration. Springer Berlin Heidelberg. https://doi.org/10.1007/978-3-642-30466-8

Shin, E.-H., 2005. UCGE Reports Estimation Techniques for Low-Cost Inertial Navigation.

Srinara, S., Chiu, Y.T., Tsai, M.L., Chiang, K.W., 2022. HIGH-DEFINITION POINT CLOUD MAP-BASED 3D LiDAR-IMU CALIBRATION FOR SELF-DRIVING APPLICATIONS, in: International Archives of the Photogrammetry, Remote Sensing and Spatial Information Sciences - ISPRS Archives. International Society for Photogrammetry and Remote Sensing, pp. 271–277. https://doi.org/10.5194/isprs-archives-XLIII-B1-2022-271-2022

Xu, W., Cai, Y., He, D., Lin, J., Zhang, F., 2021. FAST-LIO2: Fast Direct LiDAR-inertial Odometry.

Zhang, J., Singh, S., 2017. Low-drift and real-time lidar odometry and mapping. Auton Robots 41, 401–416. https://doi.org/10.1007/s10514-016-9548-2